Machinability evaluation of titanium alloy Ti-6Al-4V obtained by EBM for functional part at medical application

António Festas (afestas@ua.pt)
Universidade de Aveiro https://orcid.org/0000-0003-3335-860X

A. Ramos
Universidade de Aveiro

J. P. Davim
Universidade de Aveiro

Research Article

Keywords: turning, titanium alloys, Ti-6Al-4V, EBM, machinability

Posted Date: November 2nd, 2021

DOI: https://doi.org/10.21203/rs.3.rs-1012571/v1

Abstract

The potential and advantages revealed by the application of 3D manufacturing techniques such as Electron Beam Melting (EBM) in the production of medical devices such as orthopaedic implants are increasing manly in custom made devices. However, the use of milling and turning operations are indispensable on surfaces where surface finish and dimensional accuracy have more demanding requirements.

This work aims to evaluate the machinability of titanium alloy test samples submitted to turning operations, to obtain the geometry of a functional cone of the modular component of the hip prosthesis. The differences in cutting forces and surface finish obtained in the turning tests are compared between a wrought Ti-6Al-4V test sample and three obtained by EBM with different thicknesses. To perform the tests, a constant cutting speed of 60m/min was used, feed of 0.1 and 0.2mm/rev and a_p of 0.15mm. The cutting forces were measured for each test, also the roughness was measured in the form of R_a, R_t and R_zD in each test sample.

From the results obtained, EBM test samples presented higher roughness values and lower resulting cutting forces. In both materials, the effect of feed rate is visible. When machining a cone, the passive force and the cutting force become the most influential forces. Generally, when the feed rate value was doubled, the resulting machining forces value increased up to about 50% for both types of materials and the Ra value to approximately 200%. The EBM technology as used form medical devices allow good quality surfaces as the wrought titanium alloy.

1. Introduction

Titanium alloys, due to their properties, have a prominent place in the manufacturing of medical devices, particularly in orthopaedic implants such as screws, femoral nails [1], dental implants, components used in arthroplasty of the knee and hip joints, among others [2, 3]. Considered a bio-inert biomaterial, its low density, high resistance to corrosion, high biocompatibility and reduced Young's Modulus, compared to stainless steel and Cr-Co alloys, make them a material of high applicability to biomedical and many other applications, compared to other metallic biomaterials [4–7].

Although the use of Ti-6Al-4V alloy as a biomaterial is associated with toxicity problems related to the Aluminium and Vanadium elements, this Ti alloy is currently still the most used in the production of medical devices such as orthopaedic implants [8, 9].

In the manufacture of implants or other medical devices with complex geometries, cutting processes such as milling, turning and drilling are usually used, especially in functional areas of prosthesis. The introduction of additive manufacturing processes makes it possible to obtain complex geometries impossible to achieve with conventional manufacturing methods referred to previously. The possibility of being able to manufacture devices anatomically more compatible with the patient's physiognomy, such

as in the case of customized orthopaedic implants, translates into significant improvements in biocompatibility [10–16].

Amongst additive manufacturing (AM) processes, Electron Beam Melting (EBM), is currently one of the additive production technologies with the greatest growth in use in the manufacture of orthopaedic implants such as the acetabular component, or components used in knee and hip arthroscopy [17–20]. Compared to other AM processes, the EBM manufacturing method has highlights such as the speed of production, flexibility in the design of the component to be produced, less energy required and the obtained parts have much lower residual stresses [10, 17]. As in other AM processes, since the produced parts are near shape, the time required for finishing operations by machining is greatly reduced, comparatively if the part to be machined had to be made from scratch [21]. Despite all the advantages introduced by the use of additive methods, according to the required surface finish or geometry, complementary finishing operations by subtractive processes in functional or iteration zones may be necessary. Also, the porosity inherent in EBM manufacturing enhances the appearance of cracks on the surface of the parts. These cracks can greatly influence the fatigue resistance of the part. The machining of these surfaces is a viable and accessible solution to eliminate these cracks and increase the component's resistance to fatigue [22–24].

The combination of these two manufacturing methods fits into the concept of hybrid manufacturing [8, 13, 15, 25, 26] where the combined use of two different manufacturing technologies, in this case, AM followed by subtractive manufacturing (SM) process. Typically, the productive cycle of a component made by an AM-SM hybrid manufacturing consists in a first phase where a near-shape object is produced by AM then is submitted to an SM, normally with the use of a Computer Numerical Control (CNC) machine in one or more finishing operations, to obtain the desired geometry with higher definition, a geometric tolerance or a surface quality that can't be produced by AM. This process can be repeated as long as needed [27].

The rising demand for custom medical devices, namely orthopaedic implants, with a higher degree of biocompatibility and lower costs, reinforce the need to study the feasibility of the use of hybrid manufacturing applied to this field. Furthermore, there is a notorious lack of experimental scientific research, in this field. According to the Scopus database, under the combination of keywords "EBM" and "titanium alloys" and "machinability" only 59 papers were published from 2012 to this date. Recognizing this gap, this work carried out on an experimental basis, intends to complement the existing lack of information.

Within the scope of this work, it is intended to evaluate the machinability of the titanium alloy Ti-6Al-4V in form of EBM and wrought test samples in a current medical device application. For that purpose, the cutting forces and roughness were registered and measured in the turning of a functional geometry of a femoral cone used in the hip arthroplasty.

2. Methodology

2.1 Materials

In this work, test samples from titanium alloy Ti-6Al-4V obtained by smelting and by EBM additive manufacturing were used (Table 1). For the wrought test sample, a cylinder of 12mm in diameter with 50mm in length was used. In the case of EBM, were used four test samples, one of which was completely solid, one with a 2mm thick shell and the remaining two also with a 1,5mm thick shell. These test samples already had the near shape geometry of the cone to be obtained. The solid EBM test sample was designated as “Full” and the others were T01, T02 and T03. The test consisted of a single cutting similar to a finishing pass (a_p = 0.15mm).

Table 1
Mechanical properties of titanium alloys and test sample characteristics [10], [28], [29].

Material	**Ti-6Al-4V**	**EBM-Full**	**EBM-T01**	**EBM-T02 EBM-T03**
Geometry (mm)	Solid	Solid	Shell t=2	Shell t=1.5
E (GPa)	110	120		
YS (MPa)	680-900	950		
UTS (MPa)	780-1000	1020		
Hardness (HV)	340-350	300 - 330		
t: thickness; E: Elastic modulus; YS: Yield strength; UTS: Ultimate tensile strength				

2.2 Equipment

For machining tests, a Kingsbury Mhp 50 turning center was used. Figure 1 shows the setup in the tests performed and the detail of a test sample already machined. The geometry to be obtained is a femoral cone designated as type 10-12.

In the design of a femoral cone, the dimensions of the Cone angle (Ca), Proximal cone diameter (Pcd), Distal cone diameter (Dcd) and the Trunnion length (Tl) must be defined. Due to limitations imposed by the available material, in this case, a 12mm diameter rod, it was not possible to obtain a cone with real dimensions of the most used geometries in total hip arthroplasty [30–32]. Therefore, the 6° Ca angle was chosen equal to the 12/14 type cone, in which the 12mm dimension corresponds to the Dcd. Figure 2 demonstrates the main dimensions to be considered and an EBM machined cone, where it is possible to clearly distinguish the machined surface from the one that is obtained by the addictive process (Fig. 2).

2.3 Tools and cutting parameters

In the tests performed, a SECO Tools insert with the reference CNMG120408-MF4 TS2000 was used. According to the manufacturer, this tool should operate at average values of 60m/min for cutting speed, and 0.2mm/rev. for feed. For the tests carried out, the cutting speed was chosen accordingly to the manufacturer recommendation and for feed rate were considered 0.1 and 0.2mm/rev. since the feed rate is considered to be the most influential cutting parameter [33]. All tests were performed under dry conditions.

2.4 Cutting forces and roughness measurement

For the measurement of cutting forces, a Kistler dynamometer (Type 9121) was used. During material cutting, the components F_c corresponding to the cutting force are measured and measured on the Y-axis (Fig. 3), F_f which is the feed force and is measured in Z-axis, and the passive force F_p in the X-axis [34–36].

In the dynamometer used to measure the cutting forces, F_f, F_c and F_p correspond to F_y, F_z and F_x respectively.

To compare the cutting forces measured in each test sample, the resulting machining force F was calculated from the average values of the measured forces F_c, F_f and F_p using the following equation:

$$F = \sqrt{F_c^2 + F_f^2 + F_p^2}[N]$$

A Hommel Tester T1000 roughness meter was used for the roughness measurements, and for every specimen were made three measurements at a distance of 120° from each other. In each measurement performed, the parameters of R_a, R_t and R_zD were collected.

The traverse length considered was 4.8mm. From the results obtained was determined the average for each roughness parameter for that specific test sample. This value was then used for the analysis made.

3. Results And Discussion

3.1 – Machining forces

Table 2 shows the results of the tests. The table is mainly divided by the feed rate of each test since it was this machining parameter that differentiated the tests. The results presented are ordered in ascending order of resulting machining cutting force F. For each force output, the results of the dynamometer are divided into two types of values. The maximum force value recorded and the average of maximum and minimum force value for each axis. The average of the last two was used to determine the composition of the correspondent force. Also, in this table is presented the contribution in the percentage of each force component in the resulting cutting force that was determined with the previously referred equation.

Table 2
– Machining forces results

Material	f [mm/rev.]	F_p Avg [N]	% F_p	F_f Avg [N]	% F_f	F_c Avg [N]	% F_c	F [N]
EBM - T03	0.1	49,4	45%	19,5	18%	40,3	37%	66,7
Ti-6Al-4V		66,9	49%	24,3	18%	45,2	33%	84,3
EBM - T01	0.2	65,0	42%	23,1	15%	65,1	42%	94,8
EBM - Full		66,9	42%	23,6	15%	67,3	43%	97,8
EBM -T02		67,9	41%	25,4	15%	71,3	43%	101,7
Ti-6Al-4V		84,0	41%	37,8	19%	80,5	40%	122,3

Observing the values presented in Table 2 on the results of the cutting forces, it can be seen that there is a clear influence of the feed on the results as expected. It can be observed an increase of approximately 50% in the cutting force for the same EBM test samples geometry when the feed is doubled and of approximately 45% in the wrought test samples for the same feed variation.

As the feed rates increases, the material area with which the tool is in contact also increases. This causes a greater effort on the part of the tool to remove the material giving rise to greater cutting forces to remove that material.

In cylindrical turning operations, it is normal for the cutting force to have the most significant value, followed by the feed force and lastly the passive force. In the case of turning a cone, as in this one, it is verified by the results obtained, that it is the passive force that has the greatest impact on the resulting machining force. This is because, in this specific case, the tool moves along two axes (x and z) simultaneously. For this reason, there is a higher load on the tool along these two axes. For a 0.1mm/rev feed rate, the passive force is slightly different compared to the cutting force, in the case of a 0.2mm/rev feed rate there is a greater balance between the two.

Comparing the forces resulting from the tests carried out with feed rates of 0.1 and 0.2mm/rev, respectively (Figure 4), it is possible to notice the difference in behaviour between the two types of materials used and the consistency of behaviour for each type of material. In the wrought alloy test sample, there is a gradual increase in the resulting machining force while in the EBM test samples the machining force is stable.

In a MicroCt analysis performed on a Bruker Skyscab1275 equipment, it is possible to see the differences in consistency and density of each test sample (Fig. 5). As can be seen in the wrought test sample designated as Ti-6Al-4V in the figure, there is a uniformity in its density that is not possible to verify in the remaining test samples obtained by EBM.

From the images obtained it is also possible to identify and distinguish that the surfaces that weren't machined. These have a surface irregularity characteristic of parts obtained by 3D metal printing. This surface irregularity or discontinuity has a direct effect on the mechanical properties of the material, being directly related to a decrease in the elastic modulus and yield strength of AM parts [37]. The different mechanical properties of the materials under analysis will influence the results obtained. Therefore, it is expected for an EBM component to have lower resistance to deformation compared to a part obtained from a wrought bulk.

This can be confirmed by observing Table 2, where for EBM test samples the cutting forces are always lower than those registered for the wrought test sample. The surface discontinuity of EBM test samples offers lower resistance to the cutting tool, which, on its displacement along the surface, will find material gaps and thus be relieved of contact with the material. On the other hand, on wrought test samples, the contact of the tool with the material is continuously leading to permanent tool stress on the material.

In addition to the factors previously presented, the hardness of the material is itself a variable to take into account when interpreting the results obtained. The hardness of the tested materials, approximately 350 HV for Ti-6Al-4V and 300 to 330 HV for EBM test samples, is also the reason for the different cutting forces. A harder material is more difficult to cut, this means that a higher reaction force from the material is applied against the cutting tool during its displacement along the machined surface.

On the side of the cutting tool, there was no built-up edge formation, nor tool wear, nor chatter. Since the cutting operation was a single pass with a_p = 0.15mm that corresponds to a finishing operation in an AM part, the stress impressed over the cutting tool was minimal so that it could somehow cause any major damage to the cutting tool.

3.2 – Roughness

The machined surface of the test samples ate f=0.2mm/rev are presented in figure 6. Comparing the two images, taken with a Leica EZ4W stereo-microscope, it is possible to see that in the EBM test sample, the tool marks are more identifiable. As demonstrated before, EBM test samples required lower cutting forces, therefore, have better machinability. This means that the material offers less resistance to be removed and reacts less to the tool contact. Therefore, as a consequence of this, the tool can imprint more vividly on the EBM test sample surface its path. In wrought test samples, where hardness is superior, this results in a lesser irregulate surface or lower roughness.

The values of the R_a, R_zD and R_t roughness, measured in each test sample with a feed rate of 0.1mm/rev are presented in figure 7. From what can be observed in all measurements, the Ti-6Al- 4V wrought test sample has the lowest roughness values.

Figure 8 shows the values of R_a, R_zD and R_t, for a feed rate of 0.2mm/rev. For this feed rate value, the wrought test sample still presents the lower value.

Also, the EBM-Full test sample generally presents the lowest roughness values of the EBM set test samples. As it is more compact than the others EBM test samples, since it is filled inside, it has greater robustness than the shell type test pieces and therefore has higher deformation resistance. This implies that the component structure influence roughness values.

Regarding the measured roughness values, comparing the results of the tests with different types of feed, it is clear that for higher feed values there is an expected increase in the roughness value. This leads to the conclusion that the structure of a 3d printed part influences its behaviour when subjected to the action of a cutting tool, and that the more fragile this structure, the lower its resistance to machining. In this particular case, the result was a higher surface roughness.

Observing Fig. 7 and Fig. 8, it is clear to see the variation of the roughness parameters as the feed rate increases. For the Ti-6Al-4V test sample, there was an increase of 218% for Ra and, for the EBM test sample an increase of 180% for the same parameter.

The results obtained are consistent with the work carried by other researchers [8, 38] in which wrought test samples presented better roughness results than the EBM ones.

4. Conclusions

This work aimed, through turning tests, to access the machinability of wrought and EBM Ti-6Al-4V titanium alloy test samples. For this purpose, machining tests were carried where a cone of the hip femoral component was made and the cutting forces during machining were registered and the surface roughness was measured. From the work done, and the results obtained it can be concluded that:

- As expected, feed rate has a significant impact both on the cutting forces and on the roughness obtained. As feed rate increases, in this case from 0.1mm/rev to 0.2mm/rev, the resulting machining force increased about 50% for EBM test samples and 45% for Ti-6Al-4V alloy. Also, for the same feed rate increase, there was an increase of 218% for Ti-6Al-4V alloy and 180% for EBM test samples;
- for the feed rate of 0.1mm/rev it was possible to obtain a surface finish of grade N5 (Ra=0.4μm) that corresponds to a grinding finishing. However, given that the ISO 7206 standard states that for titanium alloys to be used in orthopaedic implants the Ra value must be 0.1μm, then it would be necessary to a complementary action of polishing to achieve the required roughness;
- the lower density of EBM test samples presents a reason for the lower machining resulting force but higher roughness values compared to wrought test samples;
- In cylindrical turning of a component, the cutting force is the one that has greater expression compared to the other forces involved. In the machining of a cone, this normal relationship between cutting forces changes, having verified in this case study, the balance between the passive force and the cutting force;
- parts obtained by EBM, after being subjected to a subtractive process as a finishing operation, can be used in applications with a high surface quality requirement. This validates the importance of

hybrid manufacturing and the use of EBM in medical applications.

Declarations

Acknowledgements

The authors acknowledge “Project No. 031556-FCT/SAICT/2017; FAMASI – Sustainable and intelligent manufacturing by machining financed by the Foundation for Science and Technology (FCT), POCI, Portugal, in the scope of TEMA, Centre for Mechanical Technology and Automation – UID/EMS/00481/2013.

The authors also acknowledge TiFast S.R.L, from Italy, for providing the Ti alloys and Mr Alex Ballu for providing the EBM test samples.

The authors also would like to thank the staff of S.mart Grenoble Alpes, G-scop (Grenoble, France) and I2M (Bordeaux, France) for the printing of the EBM parts.

Also, would like to thank PhD Suzana Pinto from TEMA, for all the help provided in MicroCT tests.

Funding: this research wasn’t supported by any funding;

Conflicts of interest/Competing interests: The authors who are involved in this work certify that they have NO affiliations with or involvement in any organization or entity with any financial interest (such as honoraria; educational grants; participation in speakers’ bureaus; membership, employment, consultancies, stock ownership, or other equity interest; and expert testimony or patent-licensing arrangements), or non-financial interest (such as personal or professional relationships, affiliations, knowledge or beliefs) in the subject matter or materials discussed in this manuscript;

Availability of data and material: Not applicable;

Code availability: not applicable;

Authors' contributions: António Festas: Experimental work, conceptualization, methodology, writing – original draft preparation; **António Ramos**: conceptualization, supervision; **J. Paulo Davim**: conceptualization, supervision.

References

1. Chen Q, Thouas GA (2015) Metallic implant biomaterials. Mater Sci Eng R Reports 87:1–57
2. Saptaji K, Gebremariam MA, Azhari MABM (2018) Machining of biocompatible materials: a review. Int J Adv Manuf Technol 97:5–8
3. Sidambe AT (2014) Biocompatibility of advanced manufactured titanium implants-A review. Materials (Basel) 7(12):8168–8188

4. Kunčická L, Kocich R, Lowe TC (2017) Advances in metals and alloys for joint replacement. Prog Mater Sci 88:232–280
5. Hussein AH, Gepreel MAH, Gouda MK, Hefnawy AM, Kandil SH (2016) Biocompatibility of new Ti-Nb-Ta base alloys. Mater Sci Eng C 61:574–578
6. Khorasani AM, Goldberg M, Doeven EH, Littlefair G (2015) Titanium in Biomedical Applications—Properties and Fabrication: A Review. J Biomater Tissue Eng 5(8):593–619
7. Kaur M, Singh K (2019) "Review on titanium and titanium based alloys as biomaterials for orthopaedic applications," *Mater. Sci. Eng. C*, vol. 102, no. February, pp. 844–862,
8. Bordin A, Bruschi S, Ghiotti A, Bucciotti F, Facchini L (2014) "Comparison between wrought and EBM Ti6Al4V machinability characteristics,"*Key Eng. Mater.*, vol.611–612, pp. 1186–1193,
9. Wysocki B, Maj P, Sitek R, Buhagiar J, Kurzydłowski KJ, Świeszkowski W (2017) Laser and electron beam additive manufacturing methods of fabricating titanium bone implants. Appl Sci 7(7):1–20
10. Harun WSW, Kamariah MSIN, Muhamad N, Ghani SAC, Ahmad F, Mohamed Z (2018) A review of powder additive manufacturing processes for metallic biomaterials. Powder Technol 327:128–151
11. Bose S, Ke D, Sahasrabudhe H, Bandyopadhyay A (2018) Additive manufacturing of biomaterials. Prog Mater Sci 93:45–111
12. Singh S, Ramakrishna S, Singh R (2017) Material issues in additive manufacturing: A review. J Manuf Process 25:185–200
13. Du W, Bai Q, Zhang B (2016) A Novel Method for Additive/Subtractive Hybrid Manufacturing of Metallic Parts. Procedia Manuf 5:1018–1030
14. Paris H, Mokhtarian H, Coatanéa E, Museau M, Ituarte IF (2016) Comparative environmental impacts of additive and subtractive manufacturing technologies. CIRP Ann - Manuf Technol 65(1):29–32
15. Flynn JM, Shokrani A, Newman ST, Dhokia V (2016) Hybrid additive and subtractive machine tools - Research and industrial developments. Int J Mach Tools Manuf 101:79–101
16. Karlsson J, Snis A, Engqvist H, Lausmaa J (2013) Characterization and comparison of materials produced by Electron Beam Melting (EBM) of two different Ti-6Al-4V powder fractions. J Mater Process Technol 213(12):2109–2118
17. Körner C (2016) Additive manufacturing of metallic components by selective electron beam melting - A review. Int Mater Rev 61(5):361–377
18. Sing SL, An J, Yeong WY, Wiria FE (2016) Laser and electron-beam powder-bed additive manufacturing of metallic implants: A review on processes, materials and designs. J Orthop Res 34(3):369–385
19. Murr LE (2015) Metallurgy of additive manufacturing: Examples from electron beam melting. Addit Manuf 5:40–53
20. Trevisan F et al (2018) Additive manufacturing of titanium alloys in the biomedical field: processes, properties and applications. J Appl Biomater Funct Mater 16(2):57–67

21. DebRoy T et al (2018) Additive manufacturing of metallic components – Process, structure and properties. Prog Mater Sci 92:112–224
22. Cronskär M, Bäckström M, Rännar LE (2013) Production of customized hip stem prostheses - A comparison between conventional machining and electron beam melting (EBM). Rapid Prototyp J 19(5):365–372
23. Liu S, Shin YC (2019) Additive manufacturing of Ti6Al4V alloy: A review. Mater Des 164:107552
24. Vo TH, Museau M, Vignat F, Villeneuve F, Ledoux Y, Ballu A (2016) "15th CIRP Conference on Computer Aided Tolerancing – CIRP CAT 2018 Typology of geometrical defects in Electron Beam Melting," vol. 00, no. 2018
25. Zhu Z, Dhokia VG, Nassehi A, Newman ST (2013) A review of hybrid manufacturing processes - State of the art and future perspectives. Int J Comput Integr Manuf 26(7):596–615
26. Lauwers B, Klocke F, Klink A, Tekkaya AE, Neugebauer R, McIntosh D (2014) Hybrid processes in manufacturing. CIRP Ann - Manuf Technol 63(2):561–583
27. Du W, Bai Q, Zhang B (2016) A Novel Method for Additive/Subtractive Hybrid Manufacturing of Metallic Parts. Procedia Manuf 5:1018–1030
28. Abdel-Hady Gepreel M, Niinomi M (2013) Biocompatibility of Ti-alloys for long-term implantation. J Mech Behav Biomed Mater 20:407–415
29. Chern AH et al (September 2019) "Build orientation, surface roughness, and scan path influence on the microstructure, mechanical properties, and flexural fatigue behavior of Ti–6Al–4V fabricated by electron beam melting," *Mater. Sci. Eng. A*, vol. 772, no. p. 138740, 2020
30. Triantafyllopoulos GK, Elpers ME, Burket JC, Esposito CI, Padgett DE, Wright TM (2016) Otto Aufranc Award: Large Heads Do Not Increase Damage at the Head-neck Taper of Metal-on-polyethylene Total Hip Arthroplasties. Clin Orthop Relat Res 474(2):330–338
31. Nassif NA, Nawabi DH, Stoner K, Elpers M, Wright T, Padgett DE (2014) Taper design affects failure of large-head metal-on-metal total hip replacements. Clin Orthop Relat Res 472(2):564–571
32. Rajpura A, Board TN (2015) The evolution of the trunnion. HIP Int 25(1):2–6
33. Rao CJ, Rao DN, Srihari P (2013) Influence of cutting parameters on cutting force and surface finish in turning operation. Procedia Eng 64:1405–1415
34. Sadílek M, Dubský J, Sadílková Z, Poruba Z (2016) Cutting forces during turning with variable depth of cut. Perspect Sci 7:357–363
35. Aslantas K, Çiçek A (2018) High speed turning of Ti6Al4V alloy in micro cutting conditions. Procedia CIRP 77:58–61
36. Stachurski W (2018) Cutting forces during longitudinal turning process of Ti-6Al-4V ELI alloy. Theoretical and experimental values. J Mech Energy Eng 2(3):201–206
37. Yuan L, Ding S, Wen C (2019) Additive manufacturing technology for porous metal implant applications and triple minimal surface structures: A review. Bioact Mater 4(1):56–70

38. Rotella G, Imbrogno S, Candamano S, Umbrello D (2017) “Surface integrity of machined additively manufactured Ti alloys,” *J. Mater. Process. Technol.*, vol. 259, no. April pp. 180–185, 2018

Figures

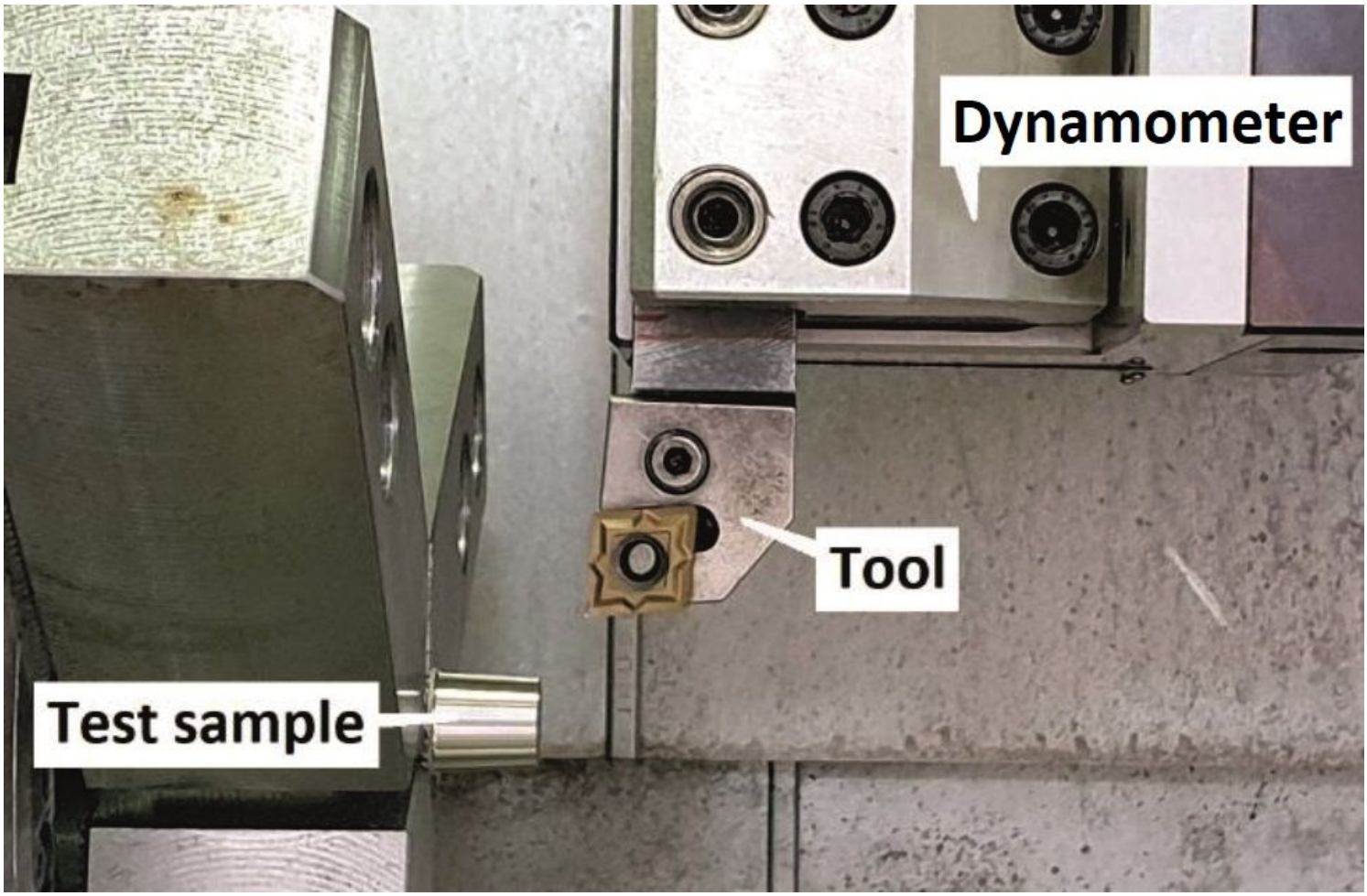

Figure 1

Experimental setup used in machining tests

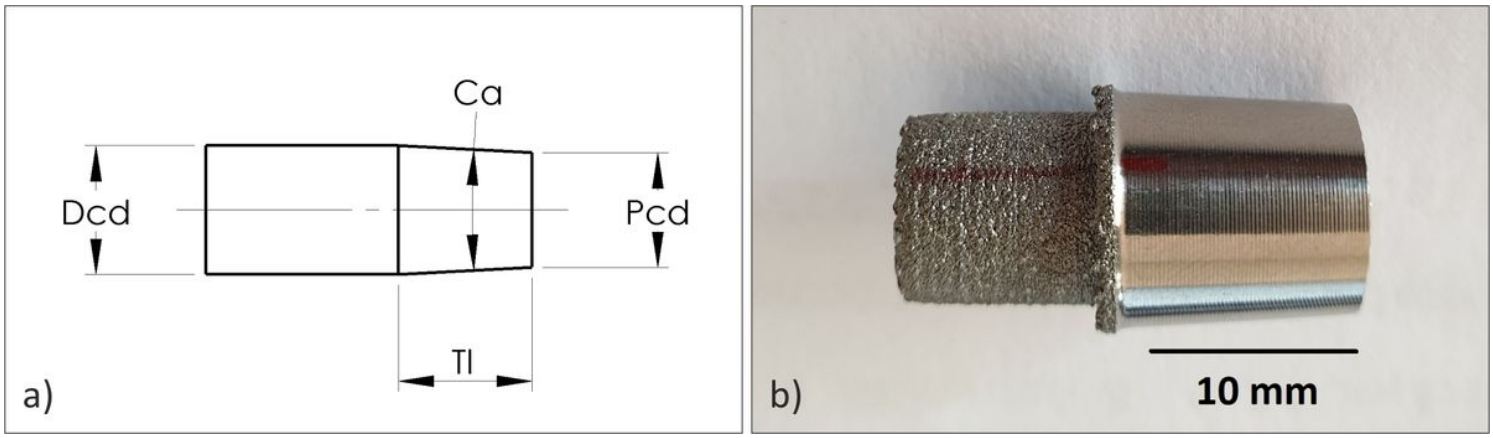

Figure 2

Cone dimensions and geometry similar to a) type 12/14 and b) a machined EBM cone

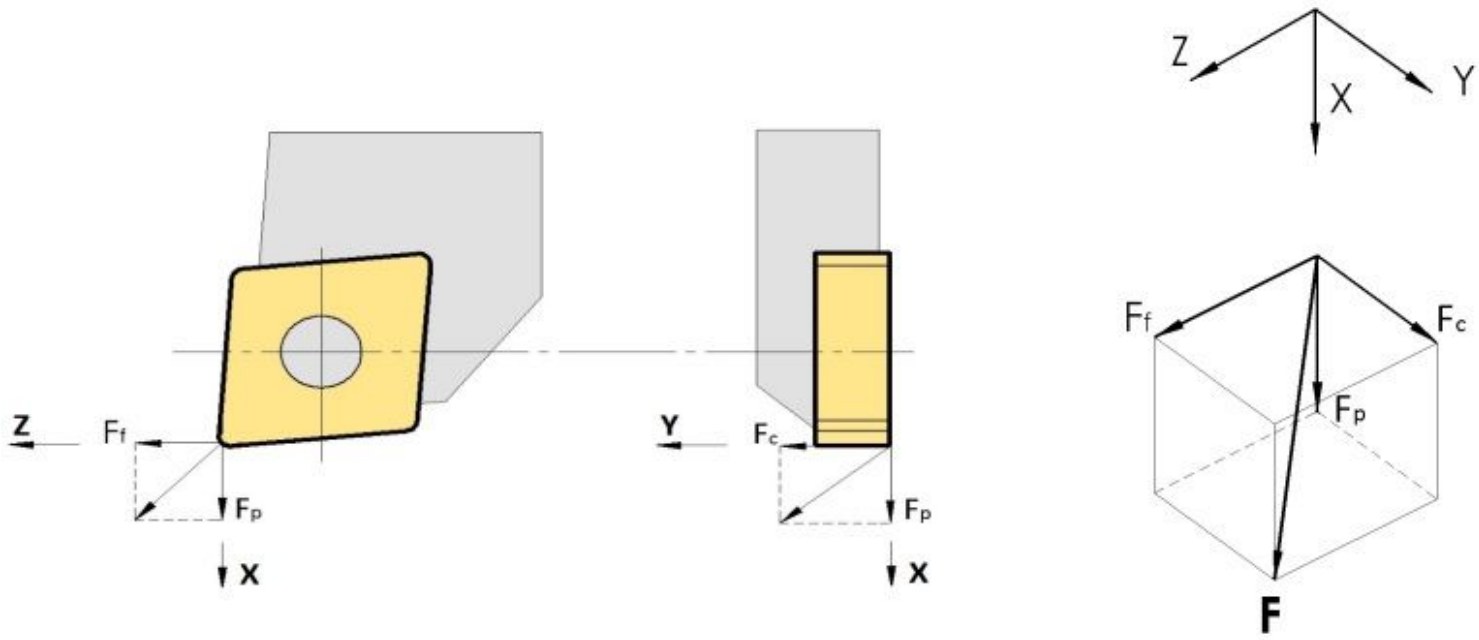

Figure 3

Cutting forces components in turning

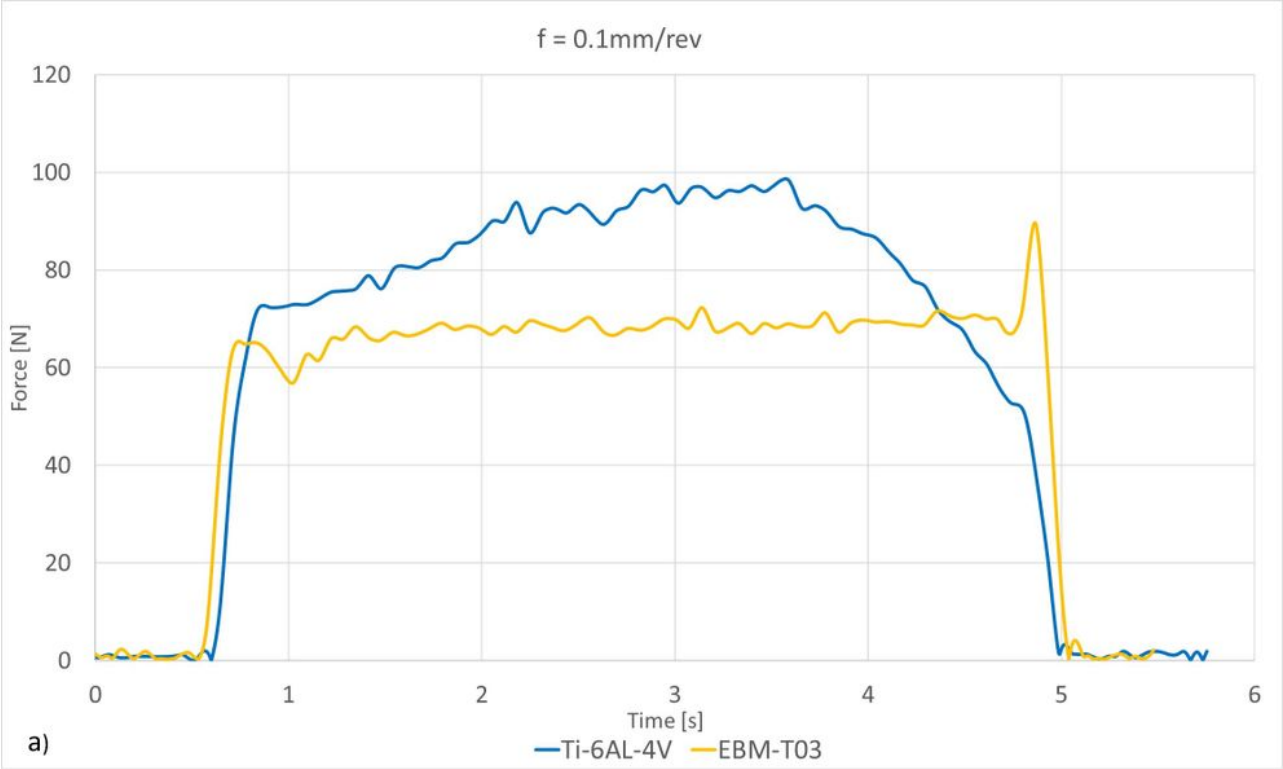

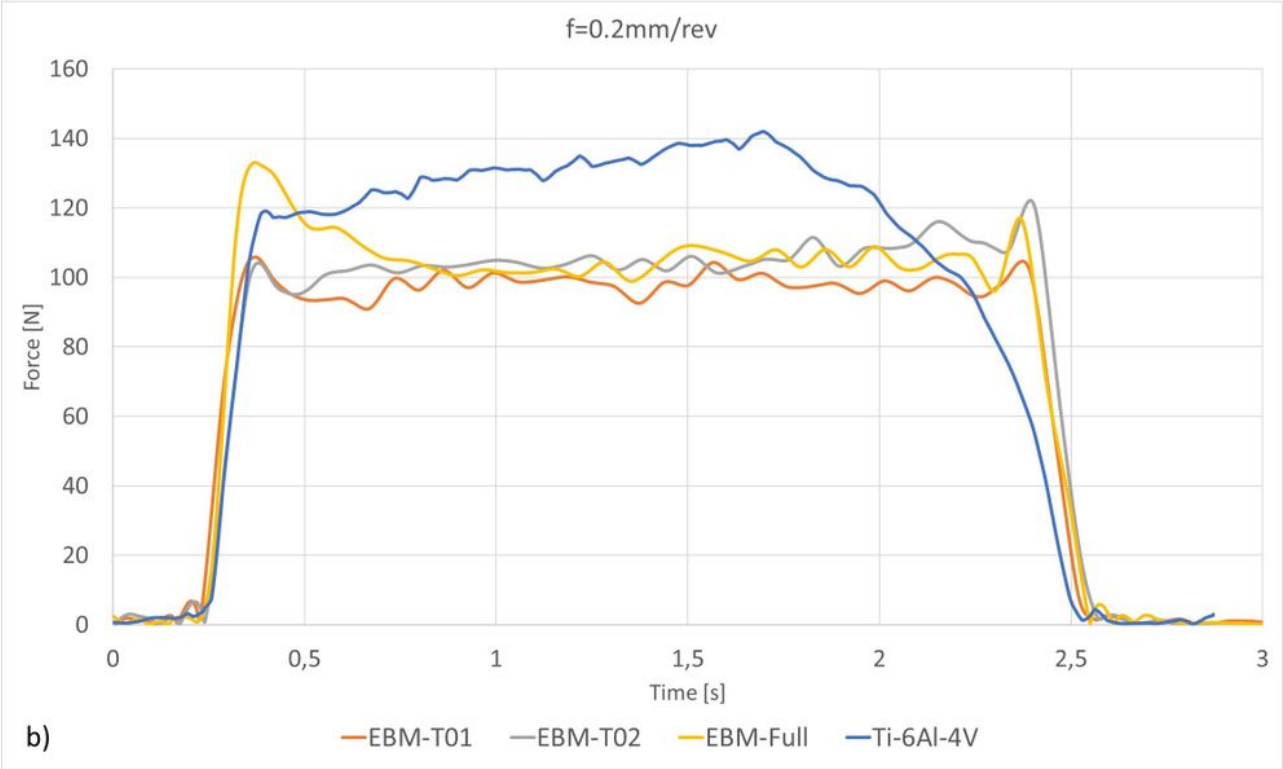

Figure 4

Resulting machining cutting force comparison for a) f=0.1mm/rev. and b) f=0.2mm/rev.

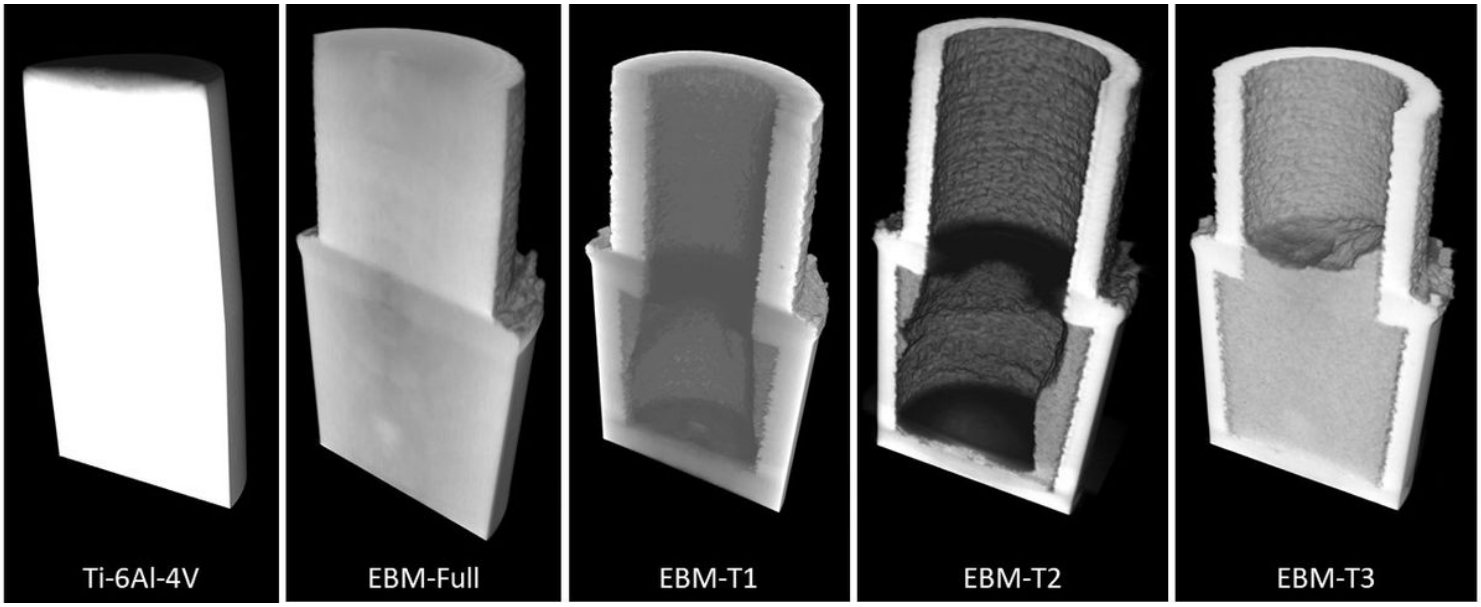

Figure 5

MicroCt analysis of the test-samples

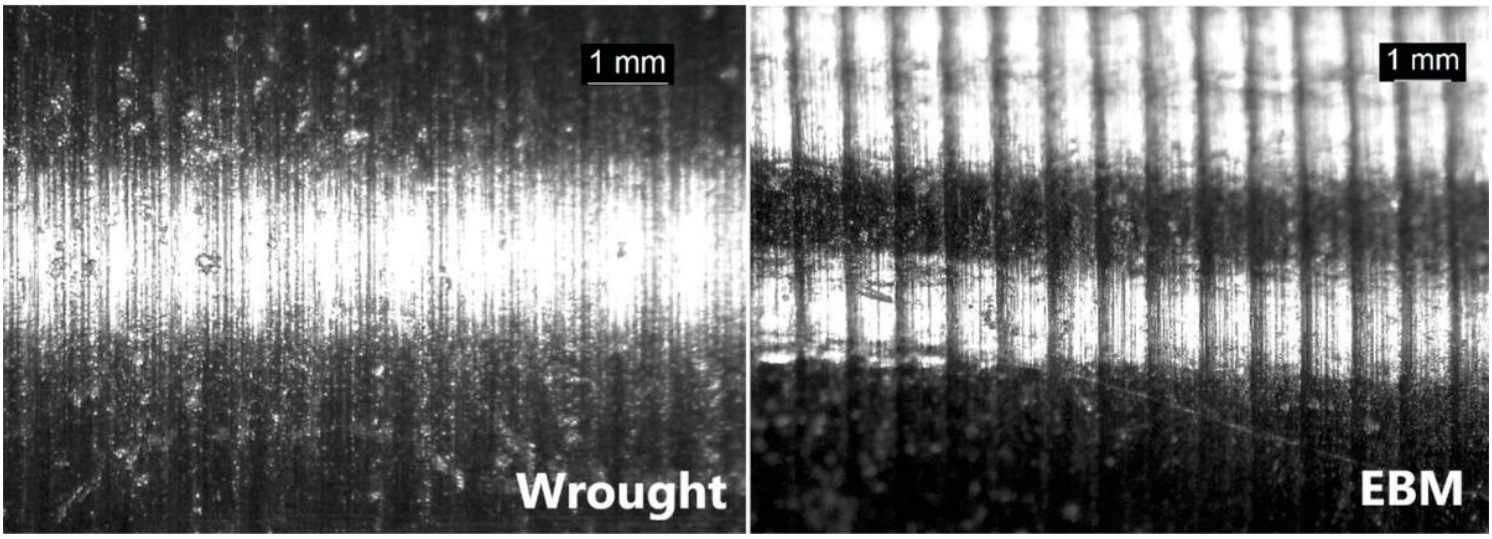

Figure 6

Wrought and EBM machined test samples (f=0.2mm/rev)

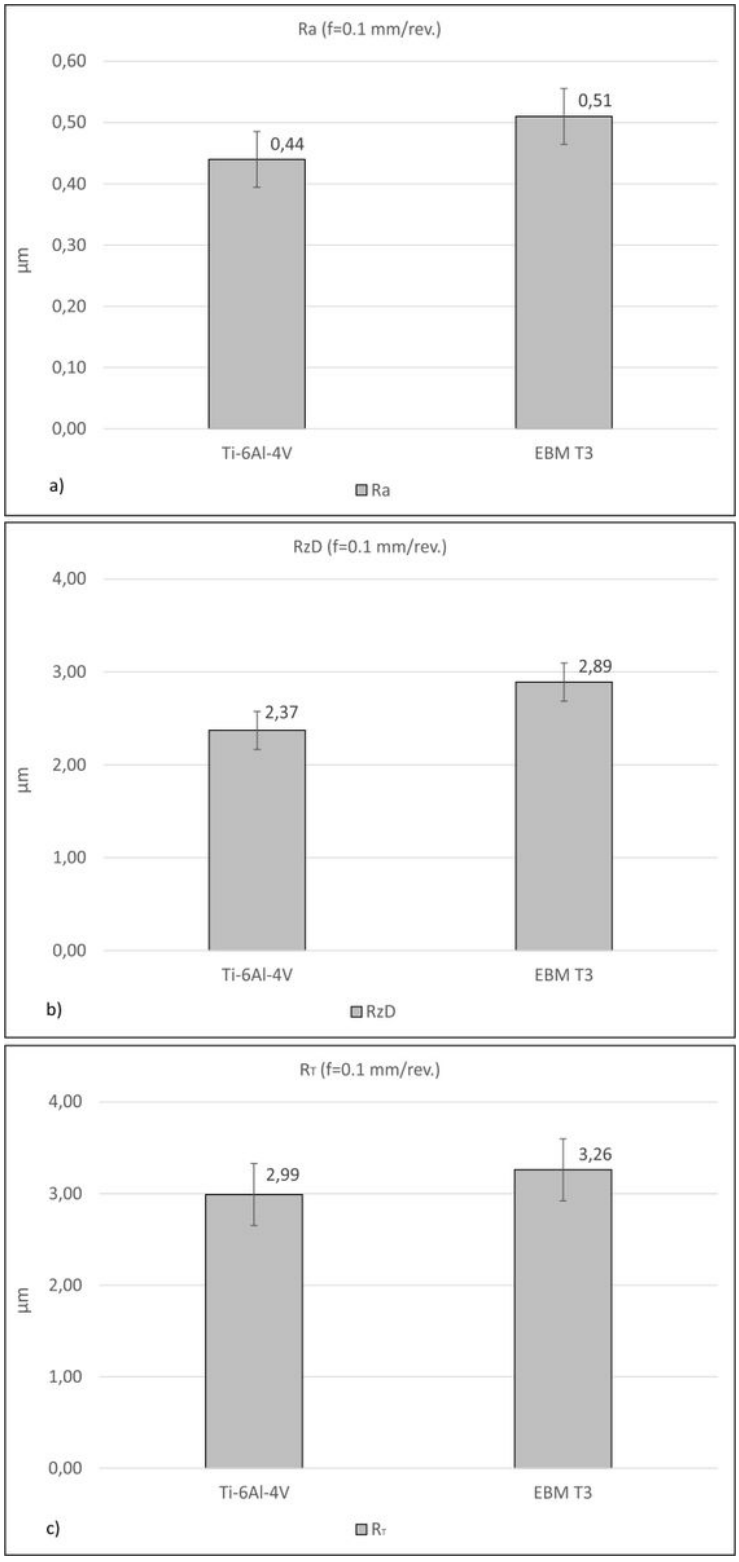

Figure 7

Roughness results for a) Ra, b) RzD and c) Rt for f=0.1mm/rev.

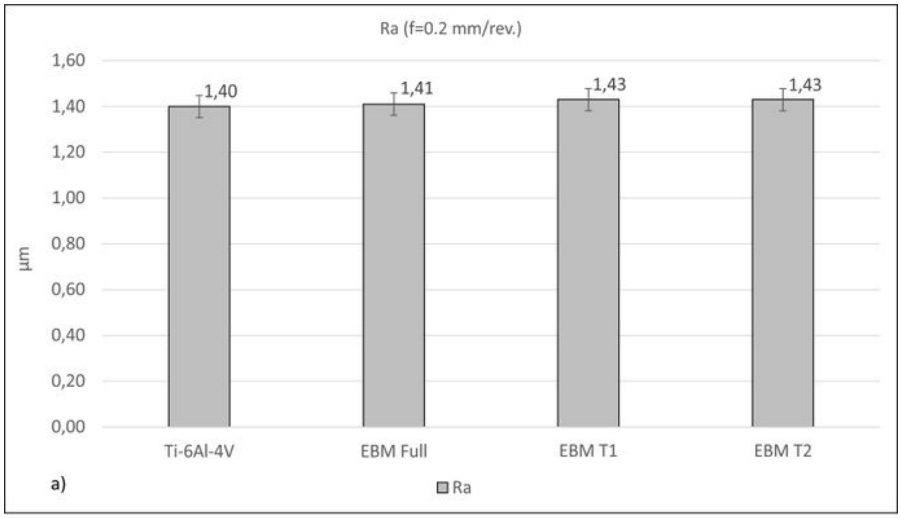

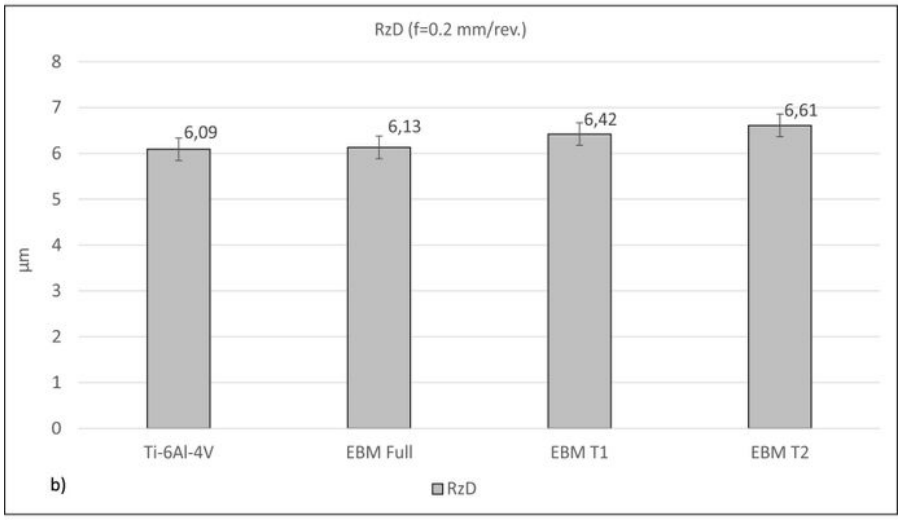

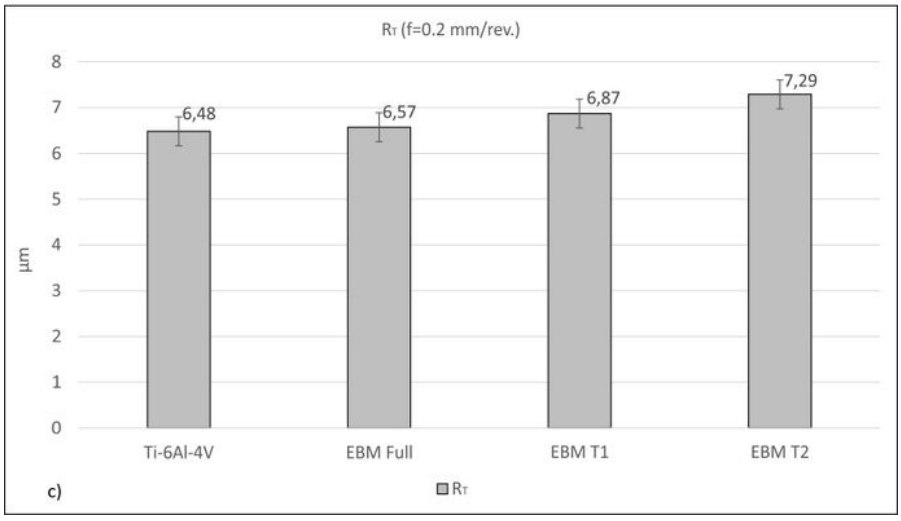

Figure 8

Roughness results for a) Ra, b) RzD and c) Rt for f=0.2mm/rev.